Texas Tech University
Multidisciplinary Research in Transportation

Novel Material Systems for the Next Generation of Flexible Pavement Structures—Phase 1 Preliminary Analysis of Field Test Data

Darryl James, Sanjaya Senadheera, Bhagya Athukorallage

Performed in Cooperation with the Texas Department of Transportation

And the Federal Highway Administration

Research Project 0-6868
Research Report 0-6868-R2
http://www.techmrt.ttu.edu/reports.php

1. Report No. 0-6868-R2	2. Government Accession No.	3. Recipient's Catalog No.
4. Title and Subtitle Novel Material Systems for the Next Generation of Flexible Pavement Structures – Phase 1 Preliminary Analysis of Field Test Data		5. Report Date October 31, 2016 6. Performing Organization Code
7. Author(s) Darryl James, Sanjaya Senadheera, Bhagya Athukorallage		8. Performing Organization Report No.
9. Performing Organization Name and Address Texas Tech University Texas Tech Center for Multidisciplinary Research in Transportation Box 41023 Lubbock, TX 79409		10. Work Unit No. (TRAIS) 11. Contract or Grant No. 0-6868
12. Sponsoring Agency Name and Address Texas Department of Transportation Research and Technology Implementation Office P. O. Box 5080 Austin, TX 78763-5080		13. Type of Report and Period Covered Phase 1 R2, September 2014 – October 2016 14. Sponsoring Agency Code

15. Supplementary Notes: Project performed in cooperation with the Texas Department of Transportation and the Federal Highway Administration.

16. Abstract

The final technical report for Phase I of this research project was divided into two parts; R1 and R2. This report R2 serves as a supplement to Report R1. Report R1 provided a detailed account of research activities conducted up to the construction of exploratory field test sections in Phase I. This report R2 provides a preliminary analysis of monitoring data collected from six exploratory field test sections. Based on early data, a seventh test section was also constructed. However, the data from that section has not been analyzed at the time of writing this report. The research team will conduct a detailed analysis of data collected from these test sections in preparation for full-scale test sections to be constructed at the Texas Tech outdoor testing site in the summer of 2017 under Phase II of this project. This research project was designed to be conducted in the following three Phases, beginning with the development of individual components and ending with the deployment of full-scale proof of concept highway projects; Phase I: Design and Demonstration (18 months), Phase II: Integration Component Demonstrations (24 months), Phase III: Final Demonstrations (12 months). Phase I was required to demonstrate any associated high-risk technologies including the use of material systems to control maximum and minimum service temperatures in the pavement surface layer, and to improve the quality and performance of layers supporting it. This is to be followed by Phase II, with integration of technologies determined to be technically viable in Phase I, while improving constructability and sustainability. Phase I concluded with the construction of exploratory field testing of novel materials system. Technical work covered in this report were carried out by seven research groups at Texas Tech University.

17. Key Words:	18. Distribution Statement No Restrictions. This document is available to the public through the National Technical Information Service, Springfield, VA 22161, 222.ntis.gov		
19. Security Classif. (of this report) Unclassified	20. Security Classif. (of this page)	21. No. of Pages 26	22. Price

NOVEL MATERIAL SYSTEMS FOR THE NEXT GENERATION OF FLEXIBLE PAVEMENT STRUCTURES – PHASE 1 PRELIMINARY ANALYSIS OF FIELD TEST DATA

by

Darryl James
Sanjaya Senadheera
Bhagya Athukorallage

Texas Tech University

Project Report 0-6868-R2

Project Number 0-6868

Performed in Cooperation with the
Texas Department of Transportation
and the
Federal Highway Administration
Texas Center for
Multidisciplinary Research in Transportation
Texas Tech University
Box 41023
Lubbock, TX 79409-1023

Products

This report contains no products.

AUTHOR'S DISCLAIMER

The contents of this report reflect the views of the authors who are responsible for the facts and the accuracy of the data presented herein. The contents do not necessarily reflect the official view of policies of the Texas Department of Transportation or the Federal Highway Administration. This report does not constitute a standard, specification, or regulation.

PATENT DISCLAIMER

There was no invention or discovery conceived or first actually reduced to practice in the course of or under this contract, including any art, method, process, machine, manufacture, design or composition of matter, or any new useful improvement thereof, or any variety of plant which is or may be patentable under the patent laws of the United States of America or any foreign country.

ENGINEERING DISCLAIMER

Not intended for construction, bidding, or permit purposes.

TRADE NAMES AND MANUFACTURERS' NAMES

The United States Government and the State of Texas do not endorse products or manufacturers. Trade or manufacturers' names appear herein solely because they are considered essential to the object of this report.

Table of Contents

List of Figures

List of Tables

1.0 Experimental Field Site – Thermal Performance

An important activity undertaken in Phase I research involved outdoor testing of pavement sections that use both conventional novel material systems. These test pavement sections were constructed at the TTU /Whitacre College of Engineering field research site. With the limited time and resources available, it was not possible to construct full-scale pavement sections for outdoor testing. Instead, instrumented test pavement sections that are sufficiently large to observe and produce meaningful data on thermal behavior were constructed at the field site. The original outdoor plan included 12 different combinations of bituminous mix and base layer designs. These are shown in Figure 1. Out of these, six test sections have been constructed with a seventh scheduled to be completed. Figure 2 identifies these six test sections. Each test section is constructed with embedded sensors to continuously monitor temperature and moisture in the layers.

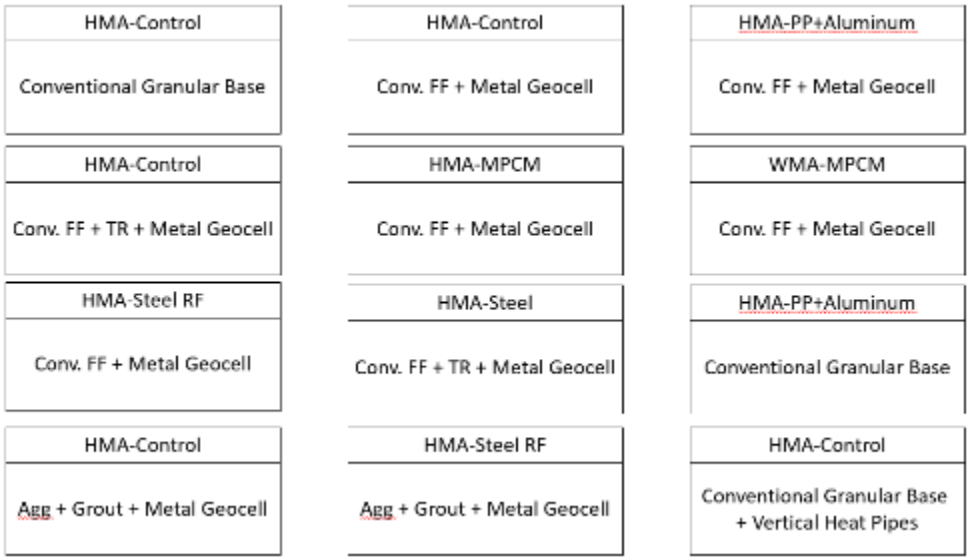

Figure 1: Exploratory Outdoor Test Sections Considered

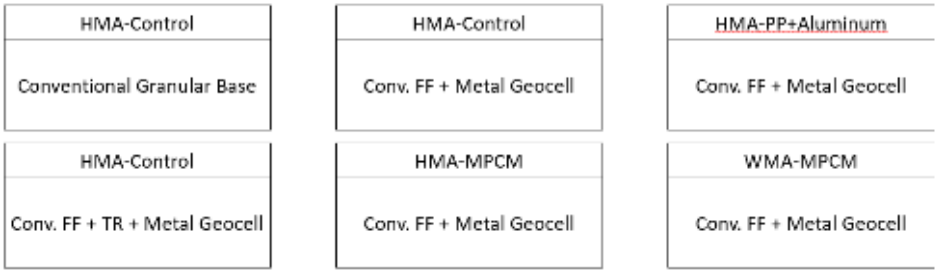

Figure 2: Exploratory Outdoor Test Sections Constructed

1.1 Field Site Hardware Setup

The data acquisition setup consists of an array of sensors, a data acquisition system, and a data storage and backup system. We have installed sensors to collect data for each test section as well as to collect thermal related data specific to the entire site.

Each test section contains 63 thermocouples distributed as shown in Figure 3. The surface layer contains the most thermocouples, 33, with the base layer containing 27. Each test section contains a heat flux gage installed on the surface near the center. The control test section contains three soil moisture sensors installed in the native soil, subgrade layer, and the base layer.

We used K-type thermocouples for the entire setup and copper wires to connect the thermocouples to the data acquisition system due to the cost effectiveness of the copper wires against thermocouple extension wires. However, because the cold junction is now moved away from the data acquisition system, cold junction compensation must be performed for each test section. We used a K-type thermocouple with thermocouple extension wire for the cold junction compensation for each test section.
Lead wires are attached to the thermocouples using isothermal blocks, and all the isothermal blocks for a given test section are placed inside an insulated PVC box located next to the test section. All copper extension wires were routed through PVC pipes into the data acquisition system located inside a nearby field site office.

In order to collect relevant surface thermal boundary condition data, a pyranometer and anemometers were installed to obtain solar insolation and near surface wind conditions. Additionally, two sensor trees that contain soil moisture sensors and thermocouples at various soils depths will be installed – one north side of the test sections and one south of the test sections following the natural grade of the land, which is generally from north to south. The purpose of the two trees is to collect "far field" thermal and moisture data. Cables from these sensors are routed to the data acquisition system either directly or through a PVC junction box located near the closest test section where applicable.

Soil moisture sensors and the cup anemometer require an external power source for operation and the pyranometer requires external power for its built-in heating element for proper operation in winter weather conditions. For all power required sensors, an external 12V DC power source was used.

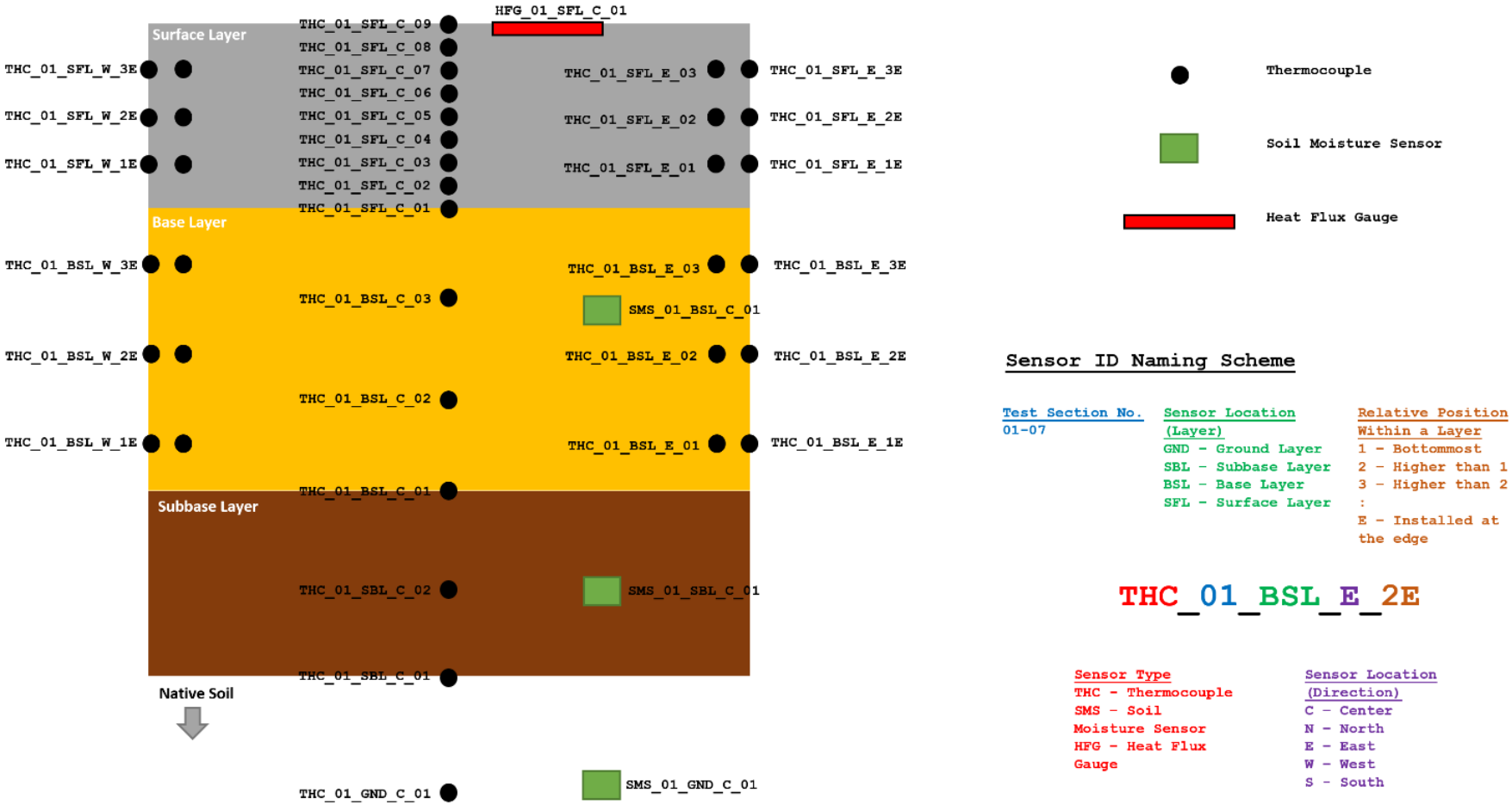

Figure 3: Overview of sensors installed in the test sections. Soil moisture sensors were not installed in the base for sections with a flowable fill base.

1.2 Data Acquisition System

The data acquisition system, shown in Figure 4, consists of National Instruments ±78 mV, Thermocouple Input, 75 S/s, 16 Ch Module (NI 9213) and 16-Channel Isothermal Thermocouple Input Modules (NI 9214) for collecting temperature data from thermocouples and National Instruments 32-Ch ±200 mV to ±10 V, 16-Bit, 250 kS/s Analog Input Module (NI 9205) for collecting data from soil moisture sensors, heat flux gages, pyranometer and the two anemometers. All modules were connected to a National Instruments CompactDAQ 14-Slot USB 3.0 chassis (cDAQ-9179) and CompactDAQ 8-Slot Ethernet chassis (cDAQ-9188).

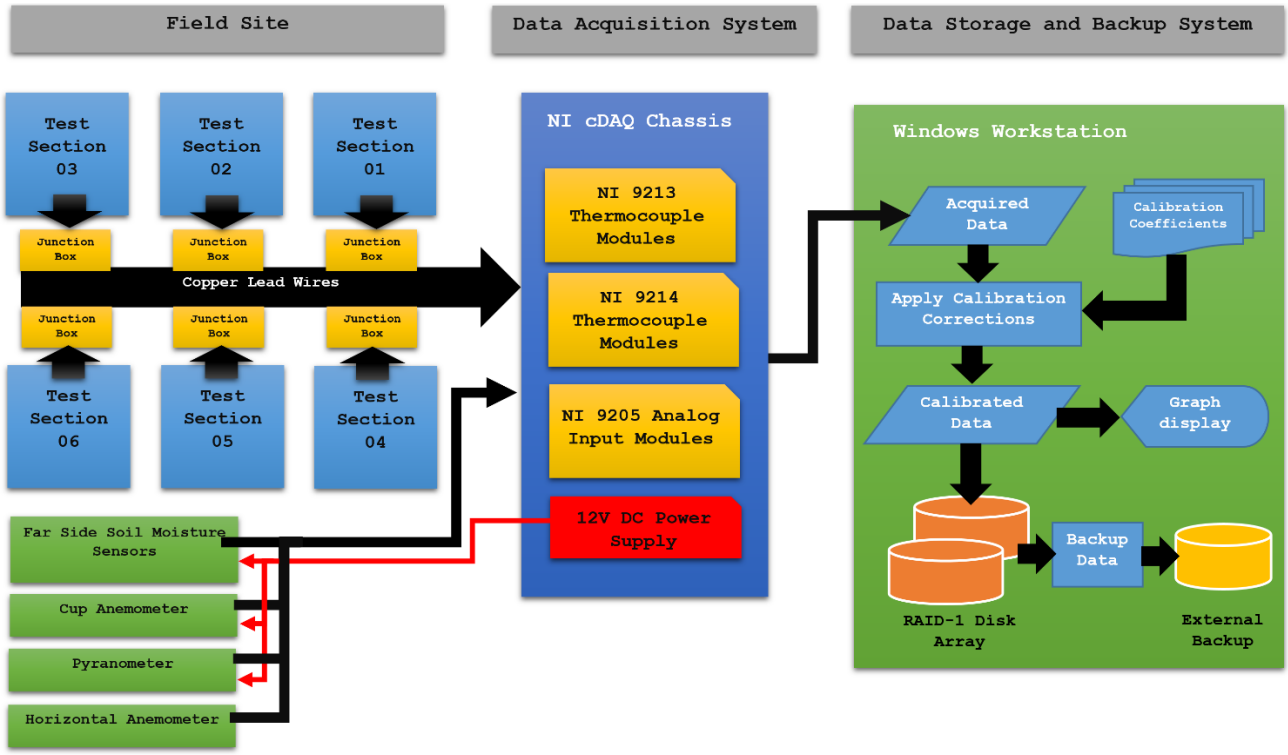

Figure 4: Block diagram of the data acquisition hardware setup

1.3 Data Storage and Backup System

A Windows-based workstation with National Instruments' LabVIEW software was used as a data collection computer. The system consists of a 10-core Intel Xeon processor with hyperthreading technology and 32GB of system memory to handle the enormous amount of parallel data acquisition processes efficiently. The data is stored in two 4-terabyte enterprise class hard drives arranged in a RAID level 1 configuration for redundancy and security. Every day after midnight, a daily backup was created on an external 4-terabyte hard drive connected through USB 3.0 interface. A weekly off-site backup copy is made for further safety of the collected data.

1.4 Calibration of Sensors

Thermocouples used in each test section were calibrated as batches in a laboratory setup. For the calibration process, the lead wires for all the thermocouples were attached and the junction temperature was compensated using another thermocouple.

All thermocouples were submerged in a constant temperature water bath and the temperature of the water bath was recorded using a precision resistive temperature device probe. Temperature readings for each thermocouple at a given bath temperature were recorded. Ten different measurements were taken for each temperature and later averaged.

Calibration coefficients were calculated by fitting a regression curve to the measured data (thermocouple readings) and the expected temperature reading (constant water bath temperature). The best fit regression curves for all calibrations were linear. These resulting coefficients from each channel were used in data acquisition setup to correct the temperature readings on the fly and record the calibrated data directly to the disk to reduce the post processing overhead.

Thermocouples used in cold junction were calibrated in the same way as the other thermocouples. The calibration data was integrated into the corresponding LabVIEW DAQ Assistant objects in the data acquisition virtual instrument for the cold junction compensation.

1.5 Development of the LabVIEW Virtual Instrument for Data Acquisition

The LabVIEW data acquisition virtual instrument (VI) consist of multiple sub-processes for thermocouple acquisition from each test section and one sub-process for all the analog sensors, including all soil moisture sensors, solar flux gages, pyranometer, and two anemometers.

Data are collected at six-second intervals and written to the disk after applying necessary calibration transformations. Note for soil the moisture sensors, heat flux gages, pyranometer, and anemometers, calibration procedures were applied using the parameters provided by the respective manufacturer.

At midnight, all recorded data are written into Microsoft Excel files and backed up.

In addition to the data collection, the LabVIEW software can display the data as it is being collected as a collection of graphs. This feature is particularly useful in viewing the current thermal conditions in each test section and also in troubleshooting sensors issues.

1.6 Experimental Thermal Data for the period October 21 – 24

We began acquiring data for all six test sections October 9th, and acquisition of the local environmental conditions on October 21st. We are in the early stages of analyzing the data, and therefore, the analysis presented will be limited, as we do not wish to make generalizations without having fully understood the data. This report presents data between October 21st and 23rd.

A weather summary during the period October 21 to 24 is provided in Table 1 for the maximum temperature, relative humidity at the time of the maximum temperature, and rain recorded within a 24-hour period. Figure 5 shows the solar heat flux and the ambient temperature as a function of time. Three of the four days experienced daytime high temperatures exceeding the "normal" highs for this time of year.

Table 1: Weather Summary (Oct 21- Oct 24)

Day	T_{max} (ºC)/(°F)	Relative humidity at T_{max}	Rain
October 21	23.7/74.7	26	None
October 22	28.2/83.3	23	None
October 23	31.7/89.1	17	None
October 24	29.6/85.3	31	None

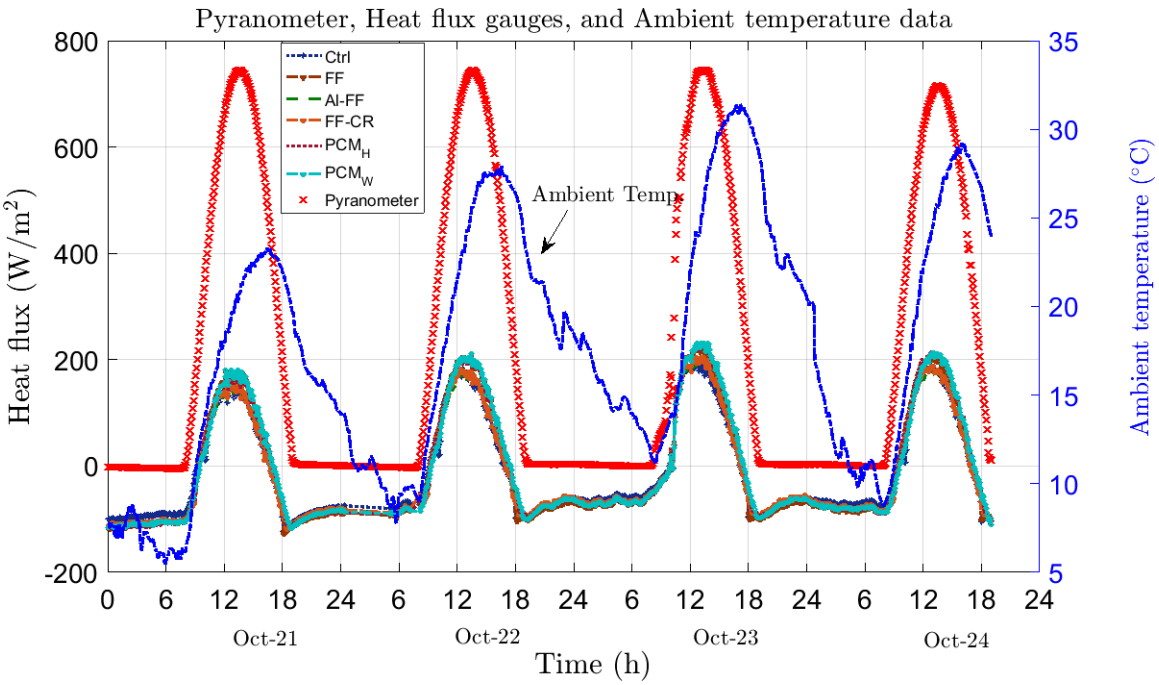

Figure 5 Solar heat flux (W/m^2) and ambient temperature (°C) as a function of time. Also shown in the heat flux gage that yields the net surface heat flux for all test sections (W/m^2).

Figures 6 - 11 show the centerline temperature variation within each section as a function of time (one minute average of data sampled 10 times per minute). The depth for each measurement is shown in the insert, where the surface is at a depth of 0 in. The thermocouple at the surface for several of the test sections did not remain fixed in place, and therefore the surface temperature data point was removed from the figures for all test sections. The ambient temperature and net surface heat flux into each test section are also shown in the figures. A positive heat flux indicates a surface net heat (radiation + convection + conduction) into the test section while a negative heat flux indicates a net surface heat flux out of the test section. The heat flux gage represents the flow of heat at the surface only.

Recall, the configurations for each test section are:

1. Test section 1 (control) – 4-inch surface layer HDMA, 8-inch conventional granular base, 4 inch caliche sub-base
2. Test section 2 – 4-inch surface layer HDMA, 8 inch flowable fill with metal geocell, 4-inch caliche sub-base
3. Test section 3 – 4-inch surface layer HDMA with 5% polypropylene, 8 inch flowable fill with crumb rubber and metal geocell, 4-inch caliche sub-base
4. Test section 4 – 4-inch surface layer HDMA, 8 inch flowable fill with x% crumb rubber and metal geocell, 4-inch caliche sub-base
5. Test section 5 – 4-inch surface layer HDMA and 50% micro phase change material of the binder content (MPCM, 43°C phase change temp), 8 inch flowable fill with metal geocell, 4-inch caliche sub-base
6. Test section 6 – 4-inch surface layer WMA and 50% micro phase change material of the binder content (MPCM, 43°C phase change temp), 8 inch flowable fill with metal geocell, 4-inch caliche sub-base

It can be seen in Figures 6 - 11 that the temperatures throughout each test section have a finite time lag when compared to the surface heat flux gage, and that the time lag increases slightly as a function of depth. The control test section has the highest near surface temperature approximately equal to 50°C, while all other test sections are at least 5°C cooler; test sections 3 and 4 show to be about 10°C cooler and test section 5 almost 14°C. It is expected that test sections 5 and 6 should show similar performance, the difference in composition between the two being the use of hot-mix or warm-mix asphalt binder. In Figure 9, a shoulder is seen in the temperature data just before 15:00 at 0.5 and 1 inch depth that indicates the phase change material (PCM) is changing phase. We would expect the same behavior for test section 5 (Fig. 8), but the temperatures do not reach the phase change temperature of 43°C. Further discussion of the temperatures in test section 5 will be made later in the report after we discuss the subgrade temperatures.

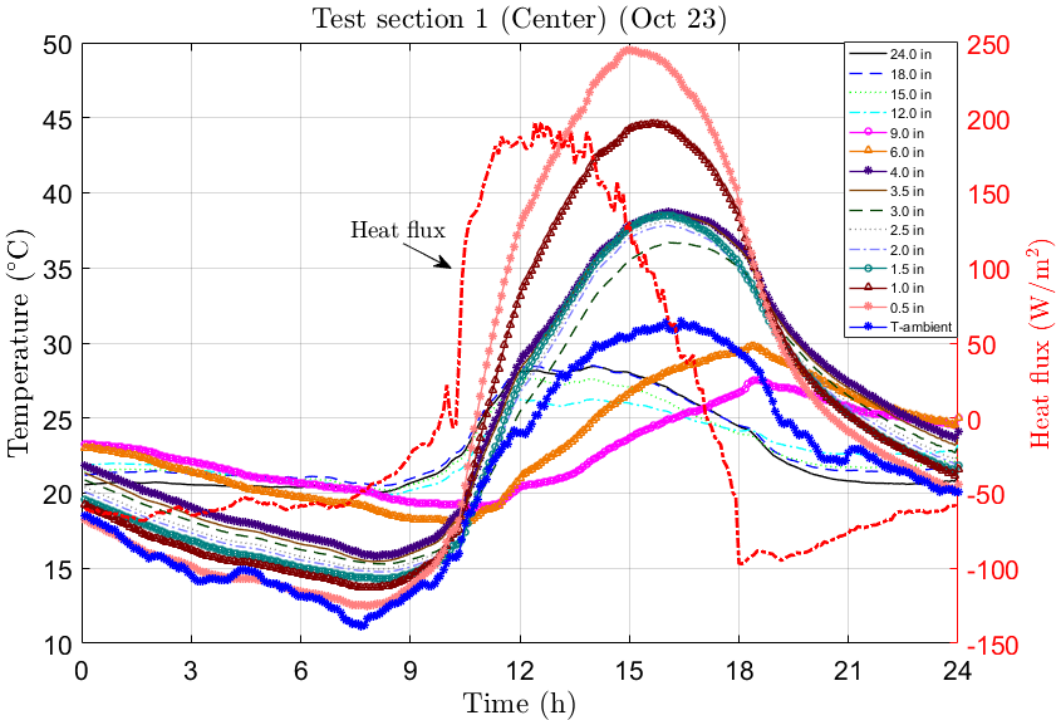

Figure 6 Centerline temperature distribution in test section 1 as a function of time. Also shown is the incident solar heat flux and ambient temperature variation with time.

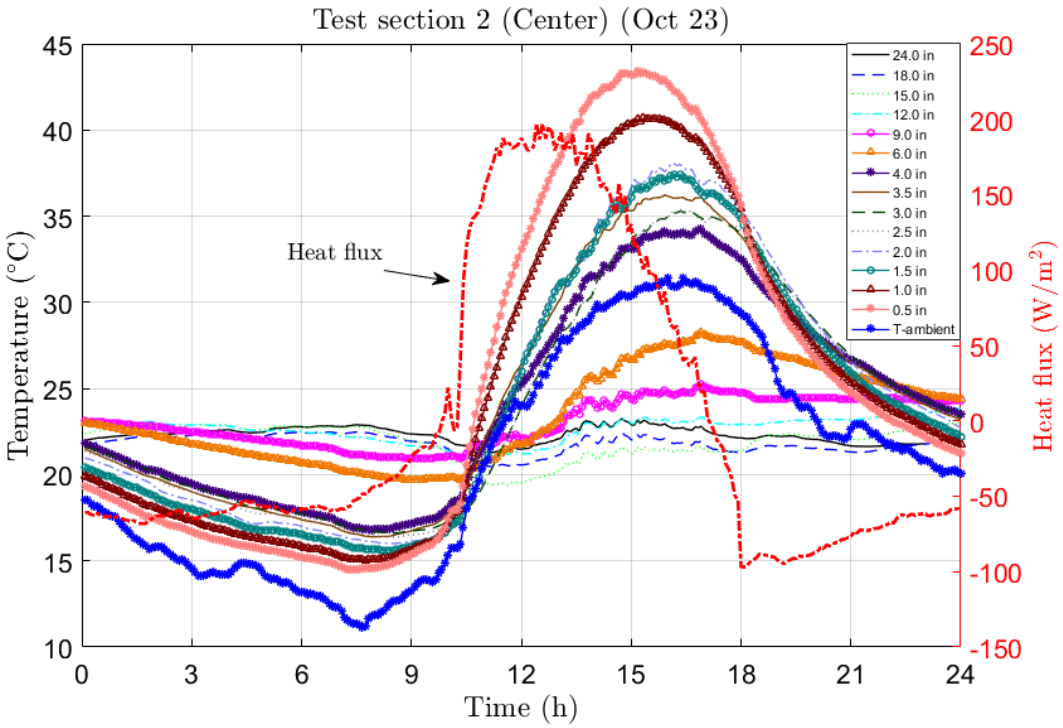

Figure 7 Centerline temperature distribution in test section 2 as a function of time. Also shown is the incident solar heat flux and ambient temperature variation with time.

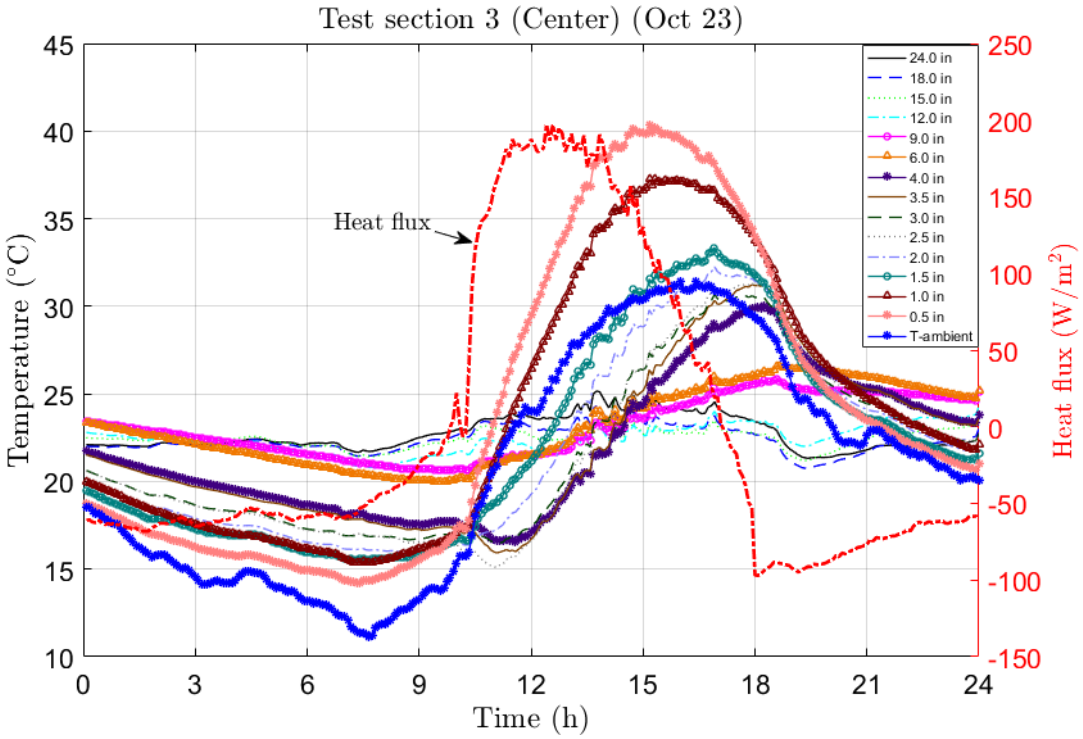

Figure 8 Centerline temperature distribution in test section 3 as a function of time. Also shown is the incident solar heat flux and ambient temperature variation with time.

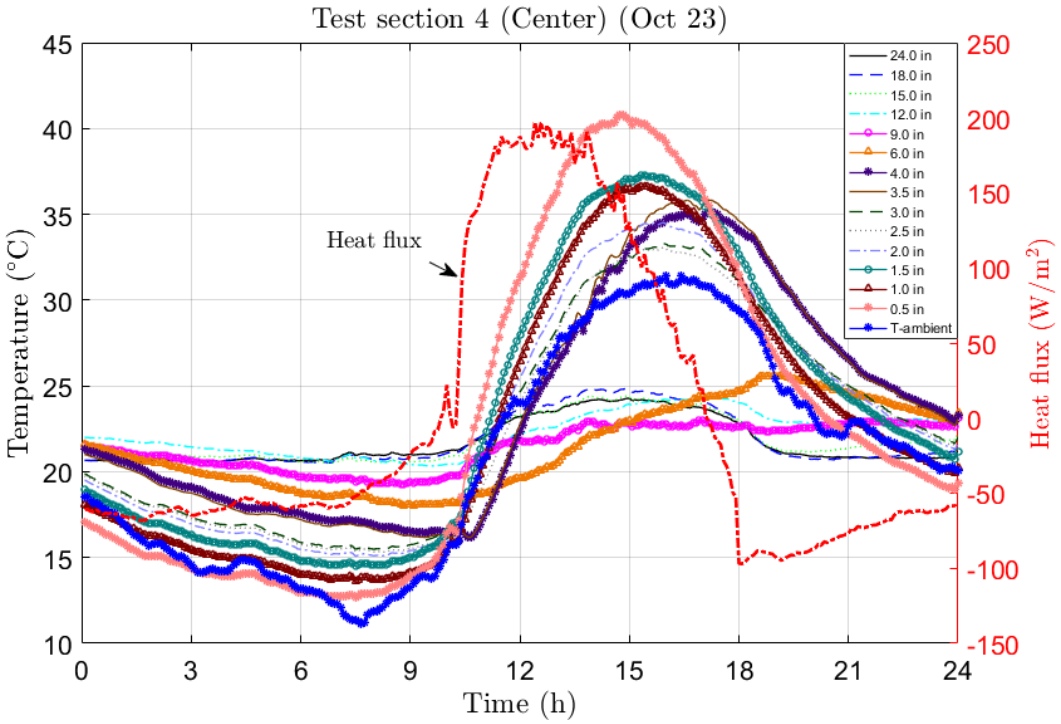

Figure 9 Centerline temperature distribution in test section 4 as a function of time. Also shown is the incident solar heat flux and ambient temperature variation with time.

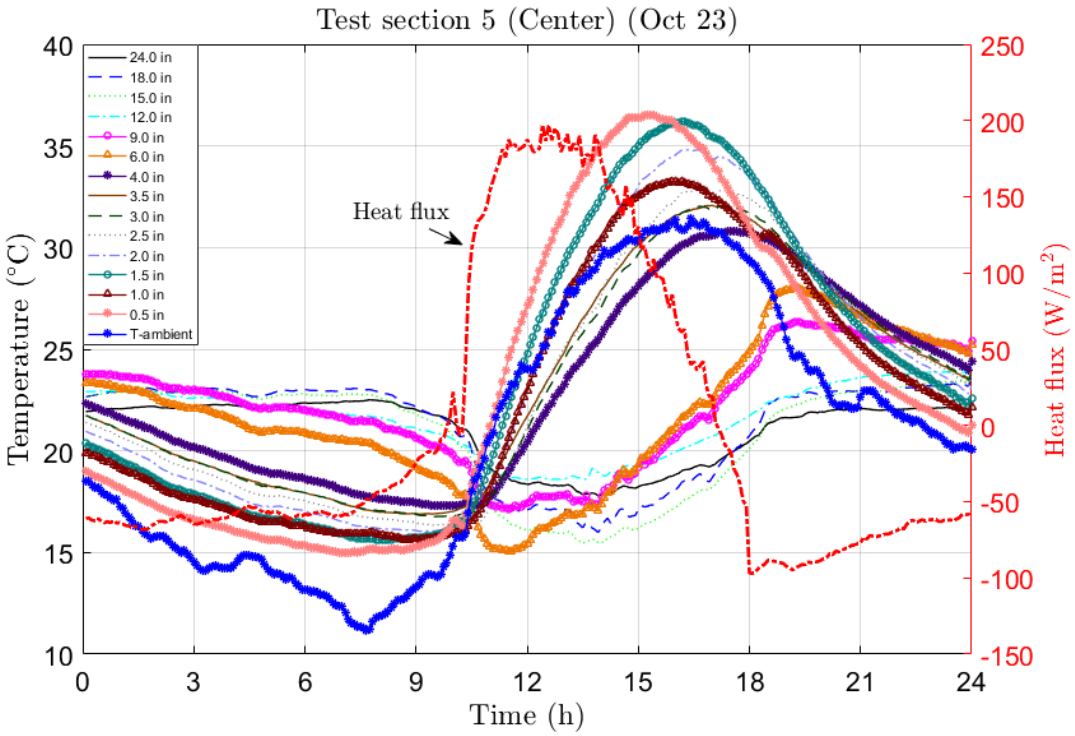

Figure 10 Centerline temperature distribution in test section 5 as a function of time. Also shown is the incident solar heat flux and ambient temperature variation with time.

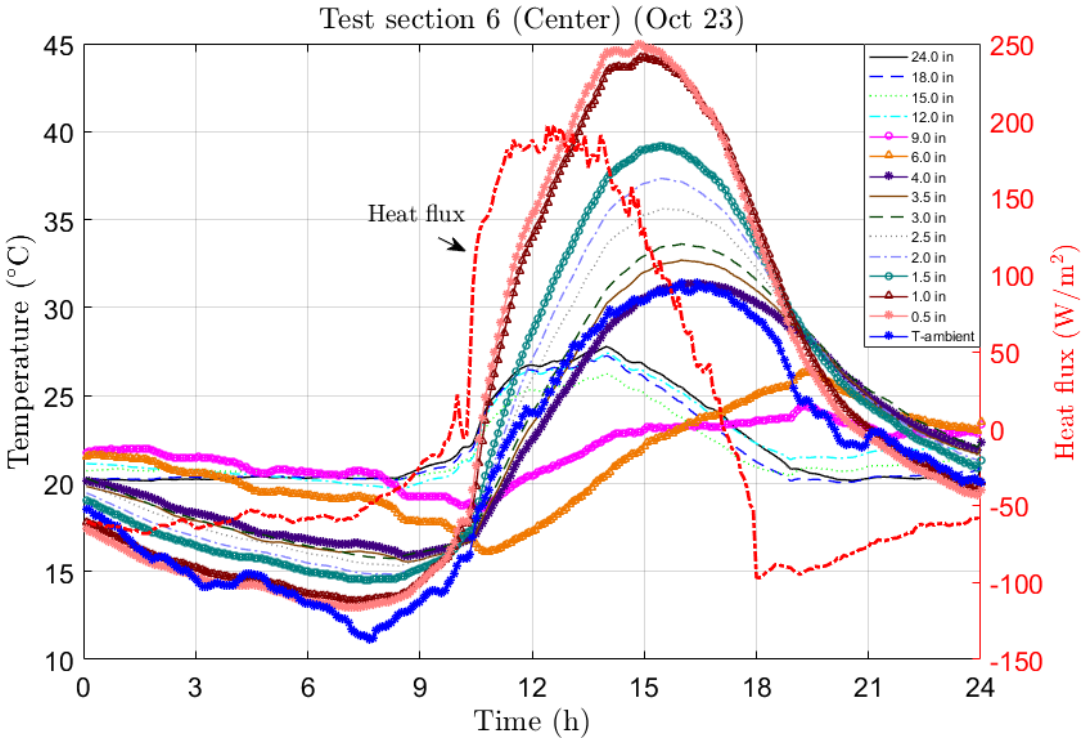

Figure 11 Centerline temperature distribution in test section 6 as a function of time. Also shown is the incident solar heat flux and ambient temperature variation with time.

We next present the vertical profile of temperature within each test section as a function of time in Figures 12 - 14 for the dates October 21st, 22nd, and 23rd. The legend inset and corresponding test section are: Ctrl – test section 1; FF – test section 2; Al-FF – test section 3, FF+CR – test section 4, PCM_H – test section 6; PCM_w – test section 6. Note at this time of year in Lubbock, sunrise is around 8 am and sunset around 7 pm CDT.

It can be seen in the figures that at 9 am the temperature distribution is such that the temperature increases with increasing depth as the solar heat input is still fairly small, and in Fig. 5 the net surface heat flux is near zero. By 10 am, enough time has passed such that the solar energy input has begun to heat the surface layer. Table 2 shows the thermal penetration depth (location where the temperature gradient changes sign), the temperature difference between the near surface and the penetration depth, and the temperature difference across the surface layer at various times after heating of the surface layer has begun (note the subscript 'PD' corresponds to penetration depth, and the subscript 'Surf' corresponds to surface layer).

Test section 3 and test section 6 have the largest temperature difference across the surface layer.

Table 2 Thermal penetration depth and the corresponding temperature difference, and temperature difference across the surface layer for a selected day (October 23, 2016).

Control (1)			
Time	Penetration depth (in)	ΔT_{Pd} (°C)	ΔT_{Surf} (°C)
9:00 AM		-4.3	-2.4
11:00 AM	1.5	7.4	5.1
1:00 PM	3	13.9	11.1
3:00 PM	6	22.6	11.6
5:00 PM	6	16.3	7.0

Flowable fill with Crumb rubber (4)			
Time	Penetration depth (in)	ΔT_{Pd} (°C)	ΔT_{Surf} (°C)
9:00 AM		-4.1	-2.5
11:00 AM	1	4.2	7.4
1:00 PM	6	16.1	10.2
3:00 PM	6	17.3	6.9
5:00 PM	6	11.5	0.9

Flowable fill base (2)			
Time	Penetration depth (in)	ΔT_{Pd} (°C)	ΔT_{Surf} (°C)
9:00 AM		-4.2	-1.7
11:00 AM	1.5	5.3	4.3
1:00 PM	3	10.6	9.9
3:00 PM	6	16.5	10.1
5:00 PM	6	11.9	6.1

PCM (Hot mix asphalt) (5)			
Time	Penetration depth (in)	ΔT_{Pd} (°C)	ΔT_{Surf} (°C)
9:00 AM		-3.8	-2.1
11:00 AM	6	6.5	3.8
1:00 PM	6	15.2	8.6
3:00 PM	6	16.7	3.1
5:00 PM	6	11.2	3.3

Asphalt layer with Aluminum (3)			
Time	Penetration depth (in)	ΔT_{Pd} (°C)	ΔT_{Surf} (°C)
9:00 AM		-4.4	-1.9
11:00 AM	2.5	8.8	7.3
1:00 PM	4	15.2	15.2
3:00 PM	4	15.2	15.2
5:00 PM	6	11.8	8.6

PCM (Warm mix asphalt) (6)			
Time	Penetration depth (in)	ΔT_{Pd} (°C)	ΔT_{Surf} (°C)
9:00 AM		-3.3	-1.5
11:00 AM	6	12.1	9.1
1:00 PM	6	21.4	14.5
3:00 PM	6	22.4	14.1
5:00 PM	6	15.7	8.6

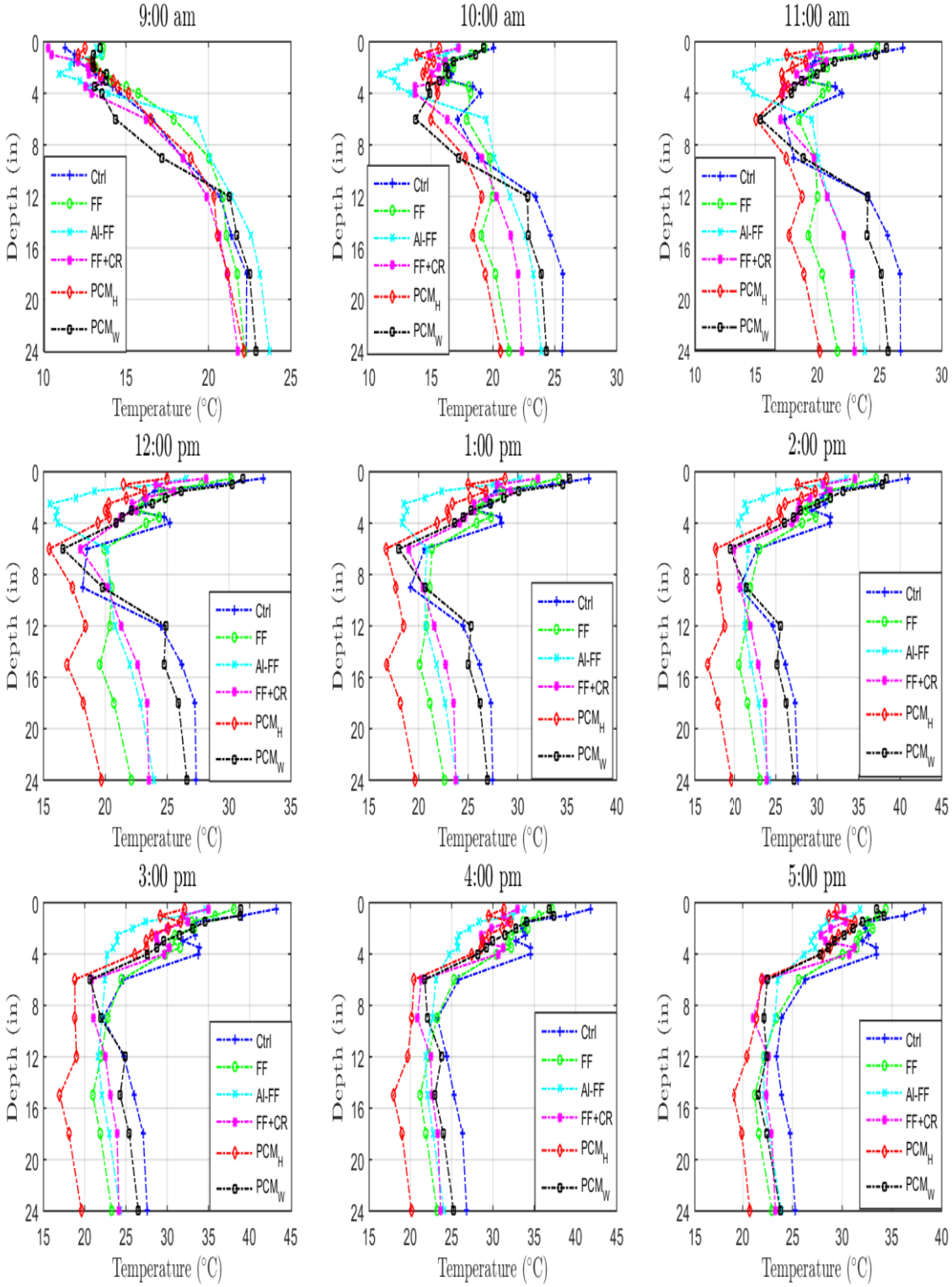

Figure 12 Centerline temperatures as a function of depth for all test sections on October 21, 2016.

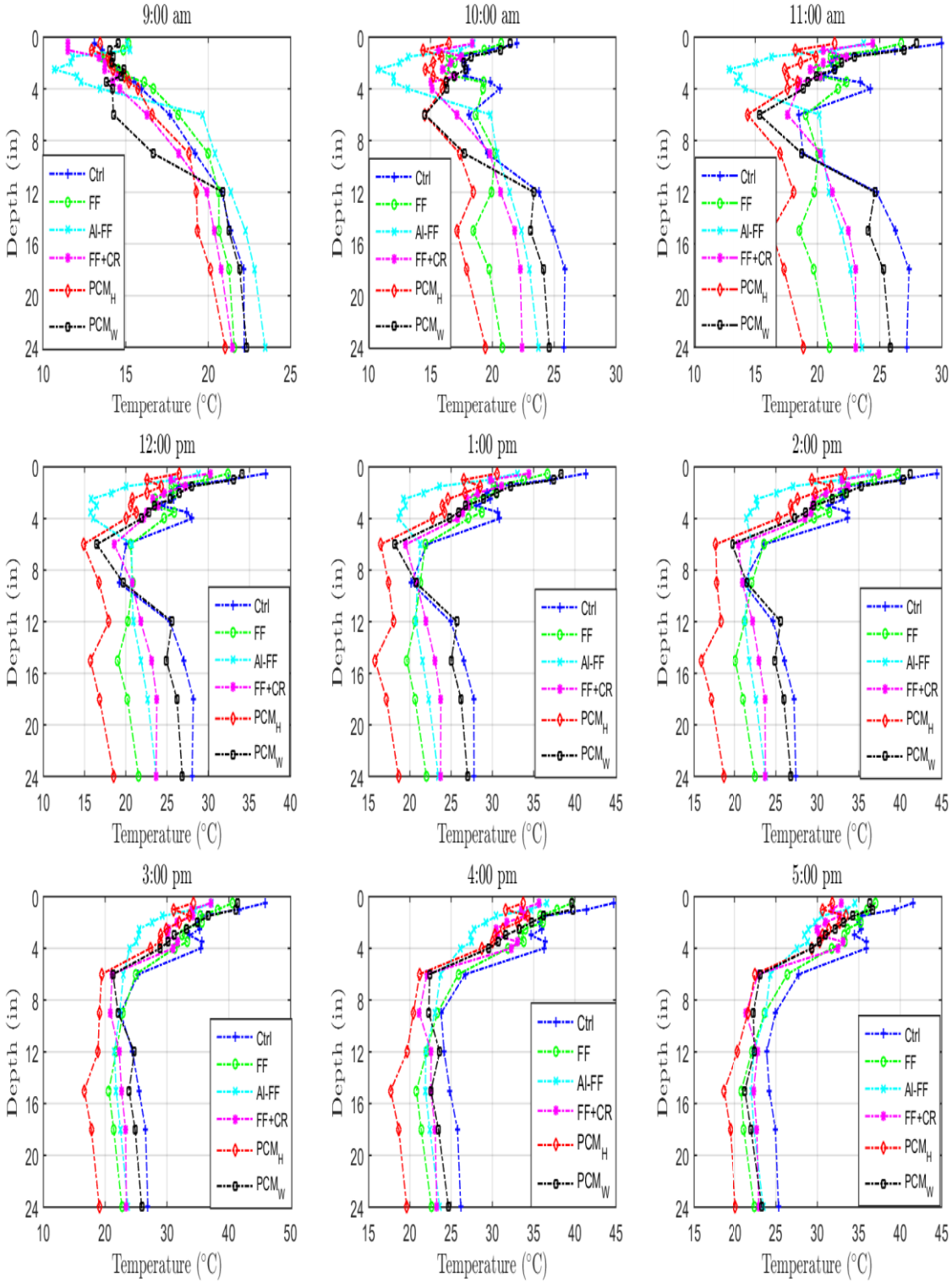

Figure 13 Centerline temperatures as a function of depth for all test sections on October 22, 2016.

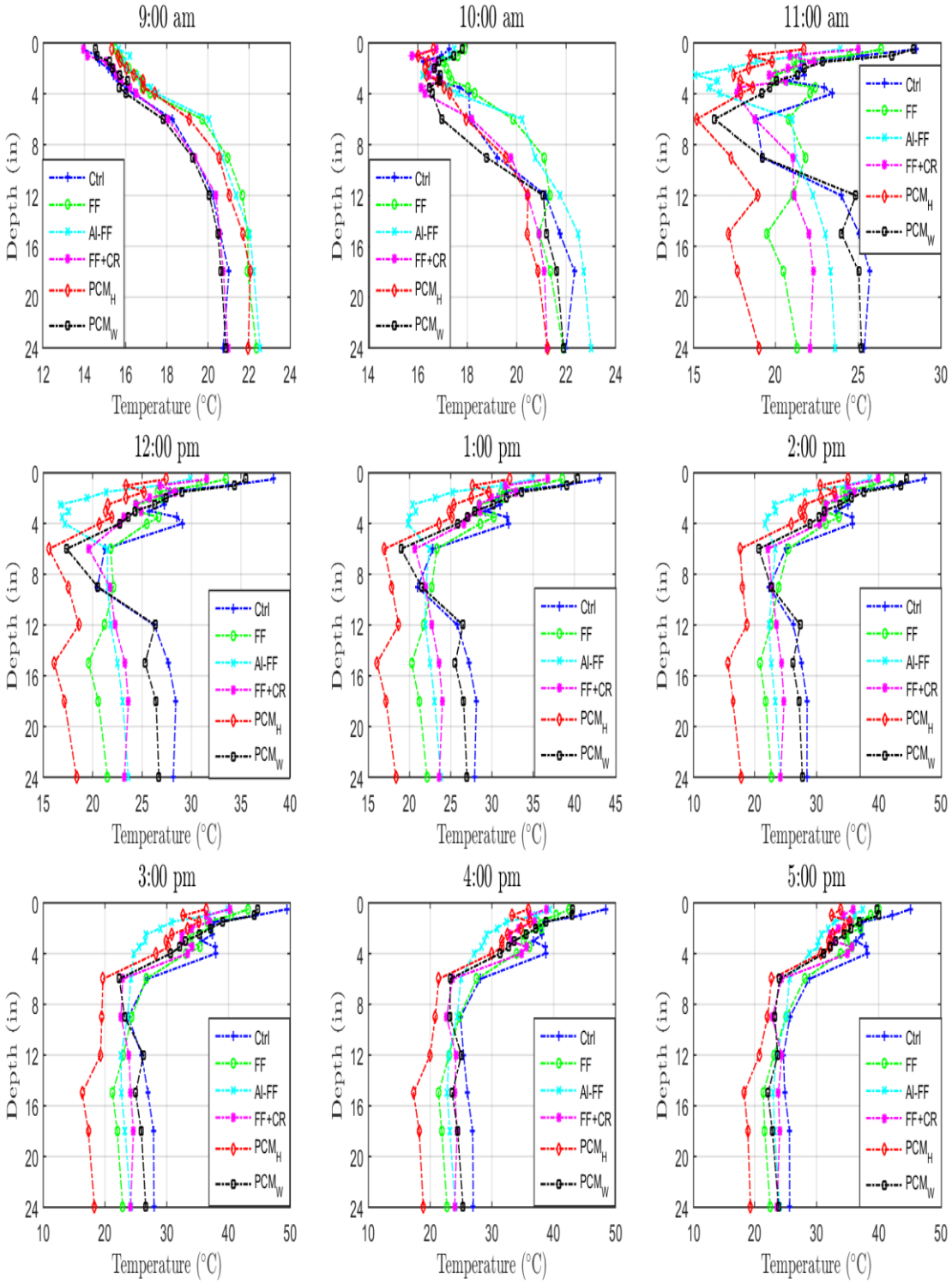

Figure 14 Centerline temperatures as a function of depth for all test sections on October 23, 2016.

In Figure 5, the net surface heat flux is shown as a function of time for each test section. Integrating the net surface heat flux over a day provides an indication of the net heat flux into (positive values) or out of (negative values) the test sections at the top surface. The net surface heat flux is given in Table 3. For the data in consideration, only October 24th showed a net positive surface flux. Interestingly, test sections 5 and 6 indicate positive surface heat flux on October 23rd, whereas the other test sections experienced a negative heat flux. Test sections 5 and 6 contain the phase change material and perhaps stored some of the thermal energy during the day to release it later; this behavior needs further investigation.

It can be seen in Figures 6 to 8 that the temperature in the caliche subgrade (24 in depth) changes with time. From a pure conduction mode, it takes on the order of a week for a change in surface heat flux to be felt at a 24-inch depth, which seems to indicate that i) the test section has a significant influence on the soil temperature eight inches below the test section and/or ii) moisture transport is present (note the moisture sensors were installed but no data was being acquired). We further investigated the subgrade temperature as a function of time for each test section to understand the variation, which is shown in Figures 15 – 20. The temperature variation in test sections 2 and 5 show a trend that is counterintuitive and opposite of the trends in the other test sections. The data for this thermocouple position indicates that the polarity may have been switched, although investigation of the connection to the DAQ module and at the extension wire connection showed this not to be the case. We are continuing to investigate. However, the temperature distribution in test section 5 (Figure 11) is compared to the subgrade temperatures shown in Figure 19, a possible reason for the reduced test section temperatures is that more heat is removed to the subgrade than the other test sections; test section 2 shows reduced subgrade temperatures similar to test section 5. The reduced subgrade temperatures under test sections 2 and 5 could be caused by moisture transport.

The last set of temperature data that is acquired that corresponds to boundary conditions on the four side surfaces of the test sections as shown in Table 4. The four sides of the test sections are labeled as North, East, West, and South as this is the direction the respective outward normal faces. At a specified depth, the mean temperature for each face, the mean temperature of the four faces and corresponding standard deviation is given in the table. The temperatures at each measured depth on the four surfaces have similar value at 9 am (i.e. the standard deviation is small in value). As the day progresses, the temperature of the side surfaces change with depth with a deviation profile that seems to follow the solar heat flux profile.

Table 3 Net energy flux through the surface (J/m^2) $x10^5$

Day	Test section 1	Test section 2	Test section 3	Test section 4	Test section 5	Test section 6
21-Oct	-1.2722	-1.3159	-1.5264	-1.4865	-1.3885	-1.2915
22-Oct	-3.6654	-2.6989	-5.5046	-5.3733	-3.5756	-3.3830
23-Oct	-1.5207	-0.3477	-1.322	-0.9895	0.7492	1.3579
24-Oct	2.3003	2.983	1.1869	1.4563	4.6775	3.6824

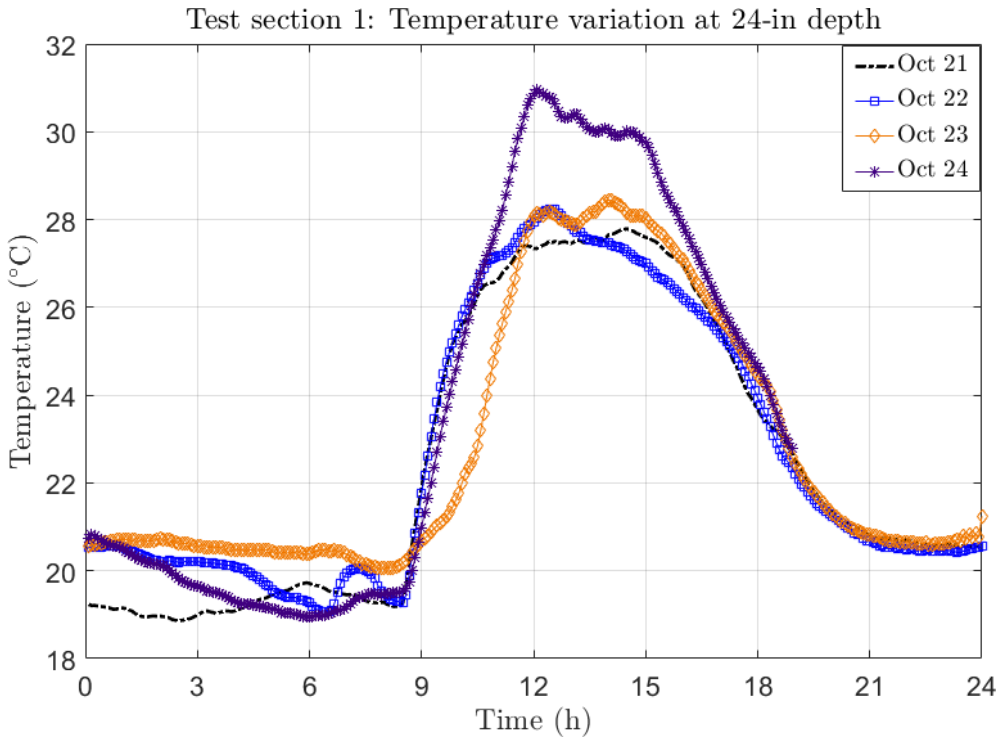

Figure 15 Subgrade temperature variation with time for test section 1

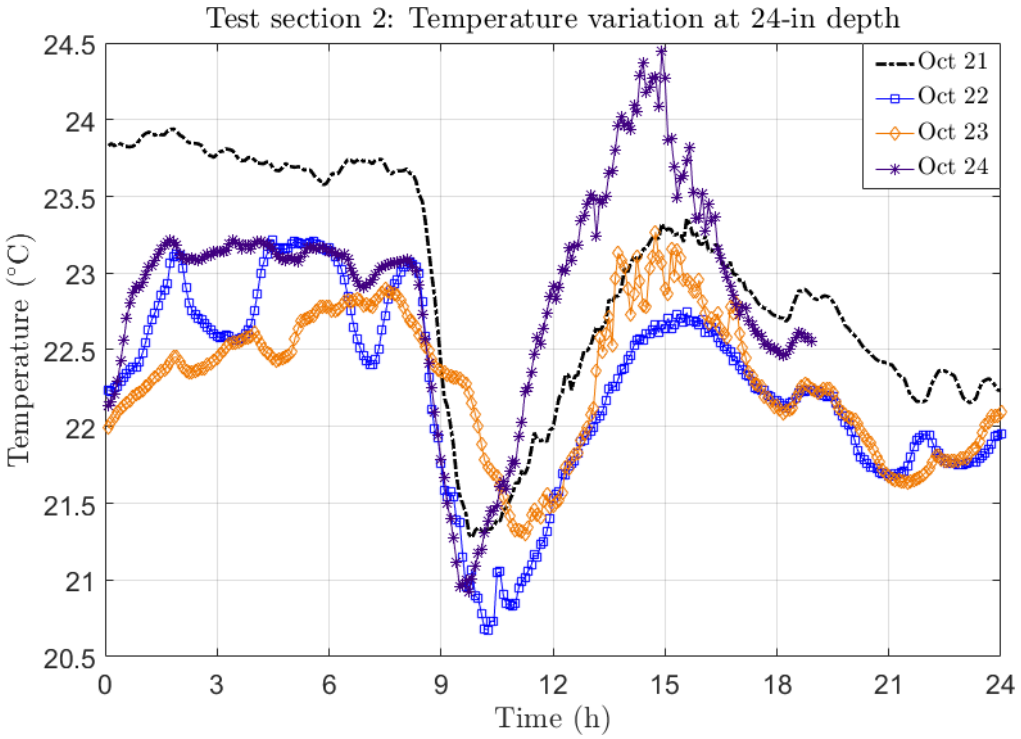

Figure 16 Subgrade temperature variation with time for test section 2

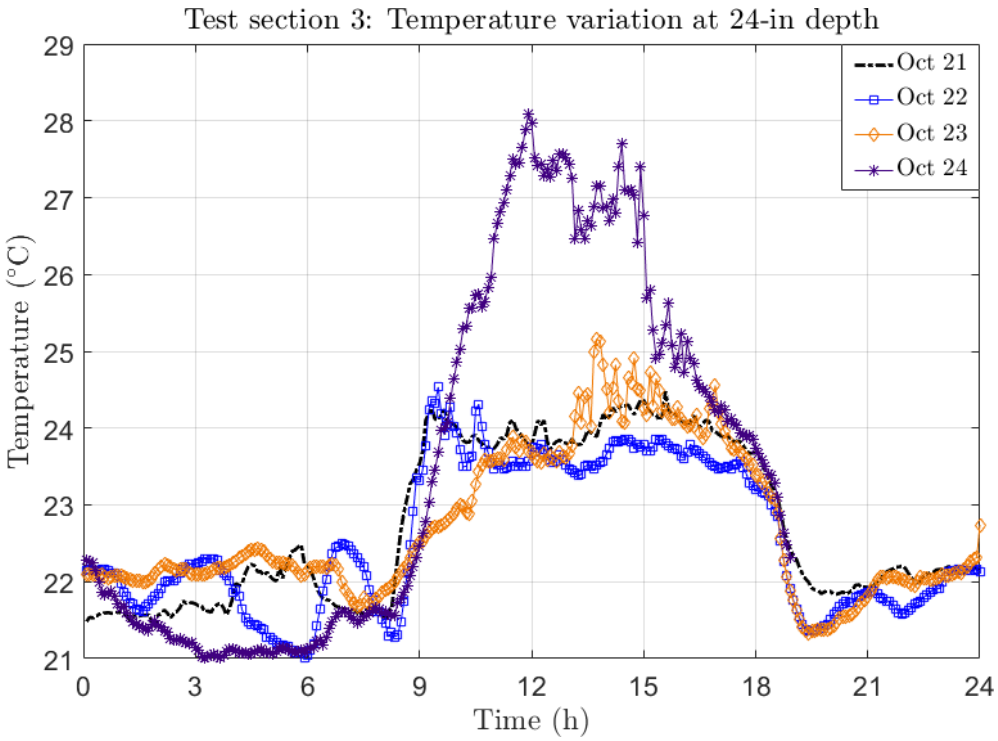

Figure 17 Subgrade temperature variation with time for test section 3

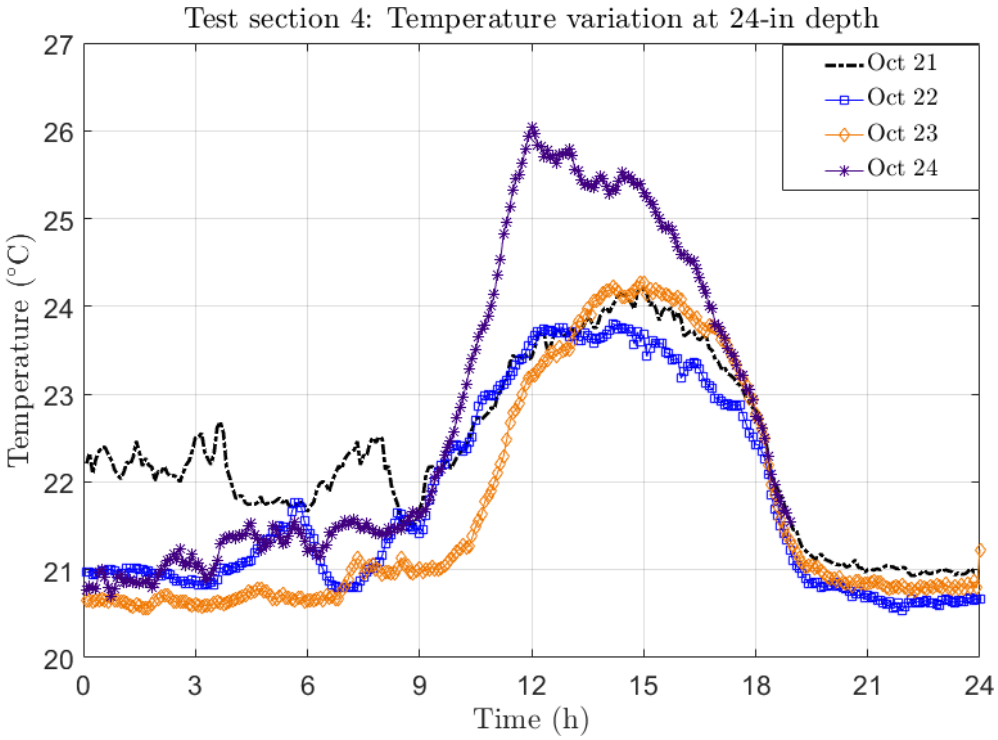

Figure 18 Subgrade temperature variation with time for test section 4

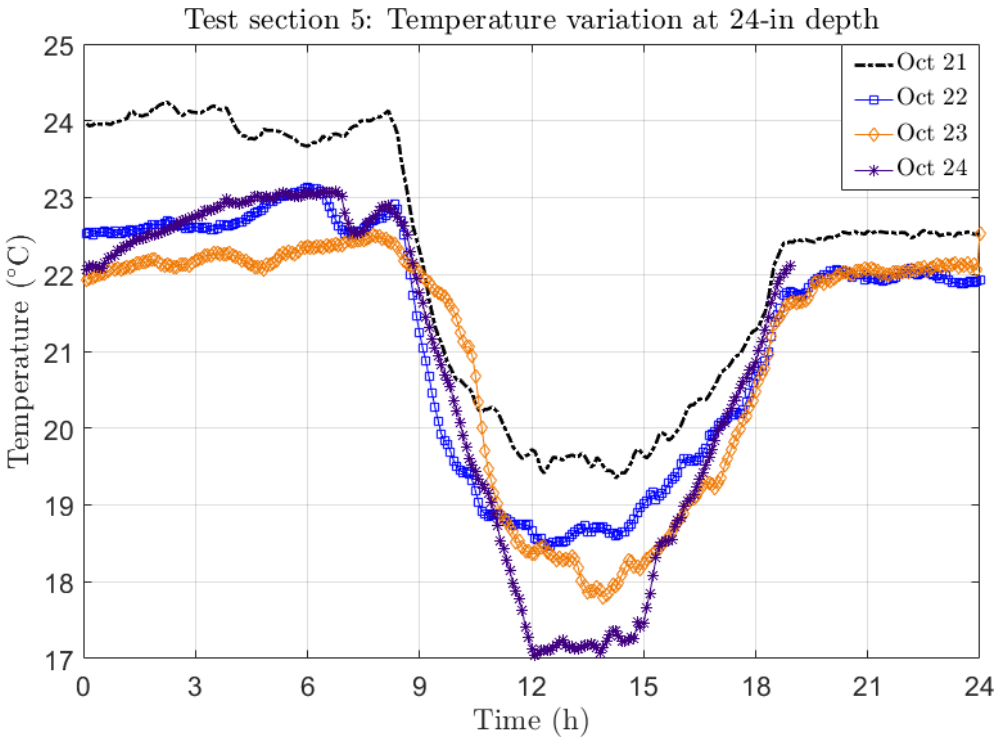

Figure 19 Subgrade temperature variation with time for test section 5

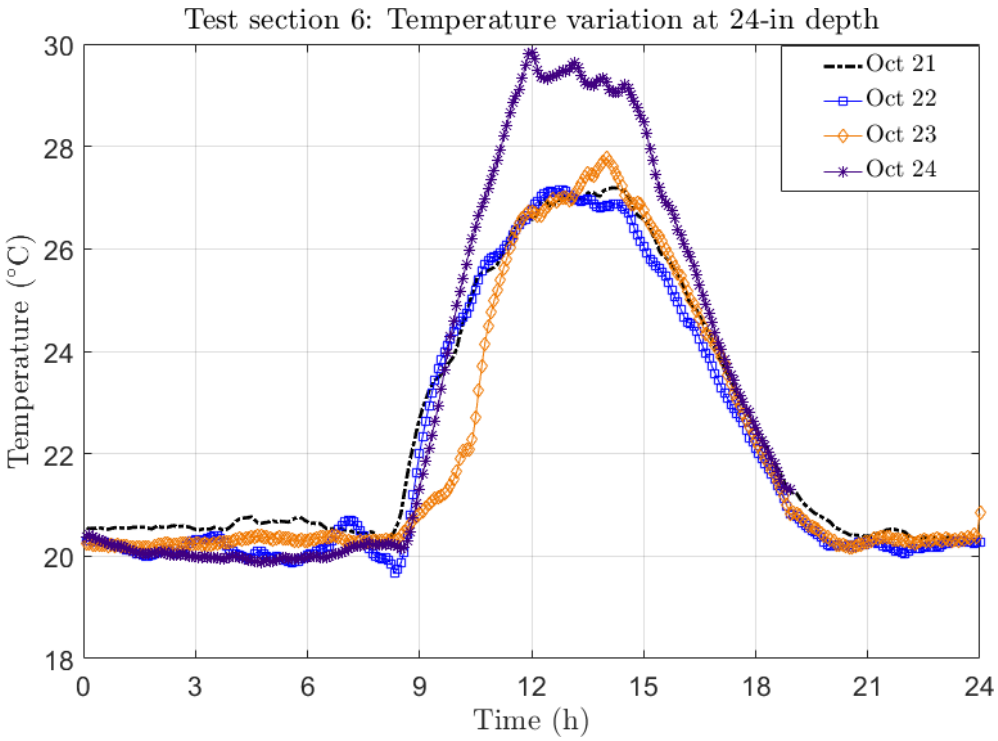

Figure 20 Subgrade temperature variation with time for test section 6

Table 4 Mean and Standard deviation for the temperature readings of thermocouples embedded on the sides of the control test section (October 23, 2016)

9:00 AM						
Depth (in)	North	East	South	West	Mean (ºC)	Standard deviation (ºC)
1	14.0	15.3	14.4	14.2	14.5	0.6
2	14.8	15.8	14.5	14.8	15.0	0.6
3	15.5	16.3	15.2	15.6	15.0	0.6
6	17.5	17.8	17.9	18.4	17.9	0.4
8	19.0	18.4	18.9	19.4	18.9	0.4
10	19.9	19.0	19.5	19.9	19.6	0.4
11:00 AM						
Depth (in)	North	East	South	West	Mean (ºC)	Standard deviation (ºC)
1	18.8	21.3	20.7	22.7	20.9	1.6
2	22.7	18.4	22.3	22.3	21.4	2.0
3	19.8	20.1	20.4	21.2	21.4	2.0
6	20.8	23.2	15.1	22.8	20.5	3.7
8	22.5	23.9	15.6	24.5	21.7	4.1
10	23.0	24.2	24.9	22.3	23.6	1.2
1:00 PM						
Depth (in)	North	East	South	West	Mean (ºC)	Standard deviation (ºC)
1	34.0	31.1	36.1	37.0	34.6	2.6
2	33.3	26.5	33.3	34.3	31.9	3.6
3	29.2	26.8	29.2	30.6	31.9	3.6
6	24.7	26.9	17.2	26.5	23.8	4.5
8	25.9	27.0	16.1	27.0	24.0	5.2
10	25.1	27.0	28.9	23.8	26.2	2.2
3:00 PM						
Depth (in)	North	East	South	West	Mean (ºC)	Standard deviation (ºC)
1	40.3	36.1	42.1	44.2	40.7	3.5
2	39.2	31.7	38.5	41.4	37.7	4.2
3	35.2	31.7	34.1	36.9	37.7	4.2
6	28.7	29.6	21.2	29.7	27.3	4.1
8	28.3	28.7	19.0	28.6	26.1	4.8
10	26.4	28.1	30.6	24.9	27.5	2.5
5:00 PM						
Depth (in)	North	East	South	West	Mean (ºC)	Standard deviation (ºC)
1	39.1	34.4	40.1	42.1	38.9	3.3
2	38.2	32.6	37.1	40.4	37.1	3.3
3	35.7	32.3	34.1	37.2	37.1	3.3
6	29.9	29.4	24.9	30.4	28.6	2.5
8	28.1	28.0	22.3	28.3	26.7	2.9
10	25.7	26.9	29.1	24.6	26.6	2.0

2.0 Conclusion

Six novel test sections have been created and instrumented for evaluation of thermal performance at a newly constructed field test site. Each test section contains 63 thermocouples distributed throughout the test section, though concentrated in the surface and base layers. Each test section contains a heat flux gage installed on the surface layer near the center.

To collect relevant surface thermal boundary condition data, a pyranometer and anemometers were installed to obtain the solar heat flux and near surface wind conditions. Additionally, two sensor trees containing soil moisture sensors and thermocouples at various soils depths will be installed.

Experimental data has been acquired from all test sections and the environmental sensors since October 21st. Thermal data over a four-day period (Oct 21 – 24) was presented to demonstrate the information being acquired to be used to evaluate the thermal performance of the six novel test sections. Initial data shows reductions in the surface temperatures for several novel configurations as compared to the control test section. However, more analysis over a longer time span is needed before definitive conclusions can be made.

TEXAS TECH UNIVERSITY
Multidisciplinary Research in Transportation

Texas Tech University Lubbock, TX 79409

P. 806.742.3503 F 806.742.4168